

Optical and Structural Studies of Phase Separation in $\text{Zn}_x\text{Cd}_{1-x}\text{Se}/\text{C}$ Core/Shell Nanocrystals

D. H. Rich¹, Y. Estrin¹, O. Moshe¹, Sayan Bhattacharyya², and A. Gedanken³

¹*Department of Physics, Ben-Gurion University of the Negev, P.O. Box 653, Beer-Sheva 84105, Israel*

²*Department of Chemical Sciences, Indian Institute of Science Education and Research, Kolkata, Mohanpur - 741252, Nadia, W.B., India*

³*Department of Chemistry and Kanbar Laboratory for Nanomaterials at the Bar-Ilan University Center for Advanced Materials and Nanotechnology, Bar-Ilan University, Ramat-Gan 52900, Israel*

Abstract. $\text{Zn}_x\text{Cd}_{1-x}\text{Se}/\text{C}$ core/shell nanocrystals with 31-39 nm diameter semiconductor cores and 11-25 nm-thick carbon shells were synthesized from solid state precursors in large scale amounts. Transmission electron microscopy (TEM) showed striations in the nanocrystals that are indicative of a composition modulation, and reveal a chemical phase separation and possible spinodal decomposition within the nanocrystals. The optical properties and carrier relaxation kinetics of the nanocrystals were examined with cathodoluminescence (CL) imaging and spectroscopy. As the excitation level is increased, carrier filling in two-dimensional phase-separated Cd-rich regions leads to a partial saturation of states before the onset of carrier filling in the higher bandgap homogenous $\text{Zn}_{0.47}\text{Cd}_{0.53}\text{Se}$ regions. In order to model the state filling and calculate quasi-Fermi levels for electrons and holes, a random quantum well model was used to determine the electron and hole eigensates in the Cd-rich regions of the nanocrystals.

Keywords: nanocrystals, ZnSe, CdSe, cathodoluminescence, transmission electron microscopy

PACS: 81.07.Bc, 78.67.Bf, 78.60.Hk

The chemical phase separation during the growth and synthesis of strained ternary semiconductors can yield additional quantum effects if the spatial modulation is less than ~ 10 nm, and possibly provide for additional device applications, such as, e.g., the spontaneous formation of quantum wires during the growth of $(\text{InP})_2/(\text{GaP})_2$ bilayer superlattices on GaAs [1,2]. Chemical phase separation within ternary II-VI crystals is a rare phenomenon, but has been predicted and observed [3].

In our recent study of $\text{Zn}_x\text{Cd}_{1-x}\text{Se}/\text{C}$ core-shell nanocrystals, TEM showed two-dimensional (2D) striations in the nanocrystals that are indicative of a composition modulation along a preferred crystallographic direction and reveal a chemical phase separation [4,5]. CL of these nanocrystals further showed that a composition modulation, Δx , of ~ 0.11 is consistent with a broadened emission and set of decomposed peaks associated with emissions from various phases in spatially integrated CL spectra [4,5].

$\text{Zn}_x\text{Cd}_{1-x}\text{Se}/\text{C}$ core/shell nanocrystals were synthesized using a simple technique of pyrolyzing the solid state precursors within a sealed reactor at higher temperatures and under autogenic pressures [4]. The

CL experiments were performed on a modified JSM-5910 scanning electron microscope (SEM) [4,5].

Figure 1(a) shows bright-field TEM images of single nanocrystals from two different regions of the sample. A hexagonal ~ 31 nm core is shielded by a ~ 8 nm carbon shell in the left image. Significant striations are observed in both nanocrystals, as seen in the figure. These striations indicate a composition modulation and spinodal decomposition within the nanocrystals, with such fluctuations occurring on a ~ 1 -5 nm size scale. In Fig. 1(b), we show spatially averaged CL spectra for $T = 60$ K over the region represented by the SEM image of Fig. 1(c). The CL spectrum was decomposed into a sum of discrete Gaussian peaks, as indicated by the labels P_1 - P_6 in Fig. 1(b). Previously, we attributed peak P_3 (564.7 nm) as due to a combination of emissions from nanocrystals possessing homogenous compositions, x , of ~ 0.47 (h) and ~ 0.50 (c), in which h and c refer to the hexagonal and cubic phases, respectively [4]. Moreover, peaks P_2 (576.2 nm) and P_4 (549.8 nm) correlate with emissions from regions exhibiting phase separation into compositions of 0.41 (h) and 0.52 (h), respectively. We have mapped the monochromatic images with wavelengths corresponding to the decomposed peaks, P_2 -

P_6 , into a composite false-color image, as shown in Fig. 1(d). We observed that groups of nanocrystals within regions of constant wavelength (i.e., false-color) exhibit very similar local CL spectra, in which the e -beam remains fixed during the acquisition of a CL spectrum.

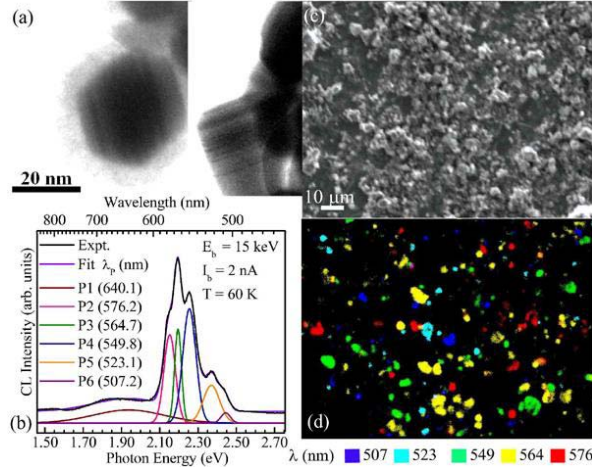


Figure 1. TEM (a), spatially integrated CL spectroscopy (b), SEM (c) and false color CL wavelength mapping (d).

Figure 2(a) shows the excitation dependence for various e -beam currents, I_b , at $T = 60$ K in a group of nanocrystals that yielded emissions for only two components, P_2 and P_3 . The e -beam was injected into a sample region size of ~ 0.1 μ m diameter for the local CL spectra of Fig. 2(a). We have quantitatively modeled the band filling in the 2D Cd-rich regions by employing a random quantum well (RQW) approximation. In this model, we assume a fixed composition modulation of $\Delta x = 0.12$, with three separate structures composed of $N_W = 4, 5,$ and 7 QWs whose well width and barrier thickness varied from 3 - 6 nm, 2.6 - 4.6 nm, and 1.6 - 3.6 nm, respectively. The total width of the multi-QW (MQW) was constrained to be ~ 36 nm, with individual well and barrier widths varying stochastically within the above three ranges for the three MQW structures. The stochastic nature of the striations in the TEM images of Fig. 1 provides the motivation for such a RQW model and is indeed consistent with observed random variations in the peak positions P_2 - P_4 , as observed in local CL spectra [4].

For a given excess carrier concentration, n_{ex} , using the two-dimensional (2D) density of states which is proportional to the appropriate in-plane effective masses, we calculated the population of each quantized state and the quasi-Fermi levels for electrons and holes, ϕ_e and ϕ_h . The electron and heavy-hole carrier densities in these quantized states can be determined by integrating the product of the 2D density of states and the Fermi-Dirac function. In this calculation, only the lowest N_W states were considered for simplicity.

The results of the band filling in the RQW model are shown in Fig. 2(b). The difference in quasi-Fermi levels, $\Delta\phi = \phi_e - \phi_h$, versus I_b and n_{ex} is shown for the three cases of 4, 5, and 7 QWs, which comprise the MQW. We also show the positions of the peaks P_2 (triangles) and P_3 (squares). A rapid increase in the intensity ratio I_{P3}/I_{P2} is observed for $I_b = 0.18$ nA. This also correlates with a ~ 10 meV shift in the P_2 component and a crossing of $\Delta\phi$ for the case of 4-QWs at the position of the P_3 peak. We observe that for the case of 4 QWs and $I_b = 0.18$ nA, a sudden increase in carrier transfer occurs when $\Delta\phi \approx E_{P3}$, the P_3 energy position, which is the position of the homogenous alloy region of $x \approx 0.46$. Thus, we conclude that for this particular group of nanocrystals, the RQW with 4 QWs yields a result consistent with carrier filling and an enhanced carrier transfer to the homogenous alloy with its concomitant increase in intensity (i.e., an increase in I_{P3}/I_{P2}) when the excitation density reaches the experimental value determined by $I_b = 0.18$ nA.

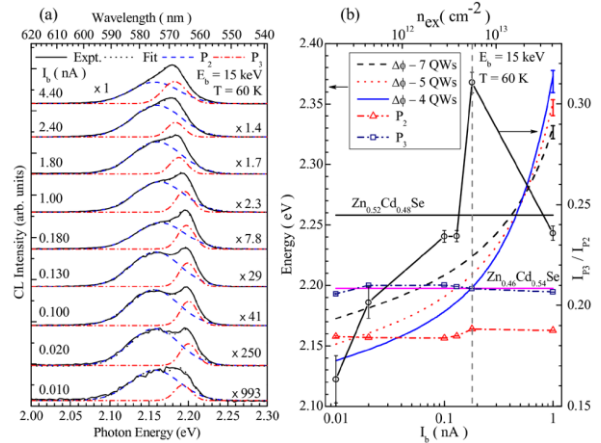


Figure 2. CL with various I_b (a) and calculation of $\Delta\phi$ (b).

In conclusion, the optical properties and the excitation-dependent carrier filling of $Zn_xCd_{1-x}Se/C$ core/shell nanocrystals with a compositional phase separation were examined with CL.

REFERENCES

1. A. Mascarenhas, R. G. Alonso, G. S. Horner, S. Froyen, K. C. Hsieh, and K. Y. Cheng, Phys. Rev. B **48**, 4907 (1993).
2. Y. Tang, D. H. Rich, A. M. Moy and K. Y. Cheng, J. Vac. Sci. Technol. B **15**, 1034 (1997).
3. A. Marbeuf, R. Druilhe, R. Triboulet, G. Patriarche, J. Cryst. Growth **117**, 10 (1992).
4. S. Bhattacharyya, Y. Estrin, O. Moshe, D. H. Rich, L. A. Solovoyov, and A. Gedanken, ACS Nano **3**, 1864 (2009).
5. Y. Estrin, D. H. Rich, O. Moshe, S. Bhattacharyya and A. Gedanken, Appl. Phys. Lett. **95**, 181903 (2009).